

IMAGING SUBSURFACE CAVITIES USING GEOELECTRIC TOMOGRAPHY AND GROUND-PENETRATING RADAR

GAD EL-QADY^{1,2}, MAHFOOZ HAFEZ¹, MOHAMED A. ABDALLA¹, AND KEISUKE USHIJIMA²

¹National Research Institute of Astronomy and Geophysics, 11722 Helwan, Cairo, EGYPT gad@mine.kyushu-u.ac.jp

²Earth Resources Engineering Department, Kyushu University, 6-10-1 Hakozaki, Fukuoka, 812-8581 JAPAN

In the past few years, construction extended extraordinarily to the southeast of Cairo, Egypt, where limestone caves occur. The existence of caves and sinkholes represents a hazard for such new urban areas. Therefore, it is important to know the size, position, and depth of natural voids and cavities before building or reconstruction. Recently, cavity imaging using geophysical surveys has become common. In this paper, both geoelectric-resistivity tomography using a dipole-dipole array and ground-penetrating radar (GPR) have been applied to the east of Kattamya at Al-Amal Town, Cairo, to image shallow subsurface cavities. The state is planning to construct a new housing development there. The resistivity survey was conducted along three profiles over an exposed cave with unknown extensions. The radar survey was conducted over an area of 1040 m², and both sets of data were processed and interpreted integrally to image the cave as well as the shallow subsurface structure of the site. As a result, the cave at a depth of about 2 m and a width of about 4 m was detected using the geophysical data, which correlates with the known cave system. Moreover, an extension of the detected cave has been inferred. The survey revealed that the area is also affected by vertical and nearly vertical linear fractures. Additionally, zones of marl and fractured limestone and some karstic features were mapped.

INTRODUCTION

Delineation of subsurface cavities and abandoned tunnels using geophysical methods has gained wide interest in the past few decades. It has been a challenging problem for exploration geophysics. The problem continues to be relevant today, as the discovery of cavities and tunnels is important to both domestic and military interests.

A variety of geophysical techniques can be used to detect the presence of caves and voids below the surface. All of them are based on a physical contrast between a cave and the surrounding rocks. Because the electrical resistance of the void is higher than the surrounding substrate, 2-D resistivity imaging is used successfully (Noel and Xu, 1992; Manzanilla *et al.*, 1994). But limestone itself has a high resistance, which means that this technique is most likely to be successful if it is used in conjunction with other methods. Palmer (1959) described an early application of the resistivity method. The difference in resistance between an air-filled cavity and the surrounding limestone may be the most outstanding physical feature of a cave, and for this reason the resistivity method has been the most widely used for cave detection (Elawadi *et al.*, 2001; Ushijima *et al.*, 1989; Smith, 1986).

Ground-penetrating radar (GPR) has been a very efficient tool for mapping shallow targets for applications such as geological engineering and environmental management (Fisher *et al.*, 1992). GPR systems detect reflections from short bursts of electromagnetic radiation emitted by a portable radar transmitter (Conyers and Goodman, 1997). Subsurface imaging by radar is possible when the topographic cover is rather smooth, and when the material penetrated is fine grained, no more than a few meters thick, and dry (Reynolds, 1997).

In the eastern part of Greater Cairo, a new housing development is planned, namely Al-Amal Town. It is about 20 km southeast of Cairo on the Cairo-Sukhna Highway (Fig. 1). The area is on the main limestone plateau that contains many intercalations of marl and clay, which are considered hazards for housing developments. Studying these areas could help the future planning for constructing new dwelling zones. Furthermore, delineating the structural patterns, fissures, joints, and faults can greatly help increase the safety factor for buildings at the study area.

The main objective of this paper is to apply both geoelectric-resistivity tomography and ground-penetrating radar to investigate the structure of a cave and to delineate any unknown caverns that might hinder future public development at Al-Amal.

SITE OF INVESTIGATION

At Al-Amal Town, the state has projected to build houses for limited-income people to be near an industrial zone. The area is located on the main limestone plateau, which contains lithologic inhomogeneities.

Stratigraphically, the shallow section in the study area and its surroundings is composed of Plio-Pleistocene deposits underlain by Pliocene and Miocene sediments. The Plio-Pleistocene is represented by feldspar-bearing coarse sand in alluvial fans of the wadies surrounding the area. The Pliocene sediments are represented by a series of gravel beds capped by a layer of white to gray, hard, and very dense limestone (Said, 1962). The Miocene section of the Cairo-Suez district increases in thickness toward the east and averages 30 m around the study area. It is divided into two main units, an upper nonma-

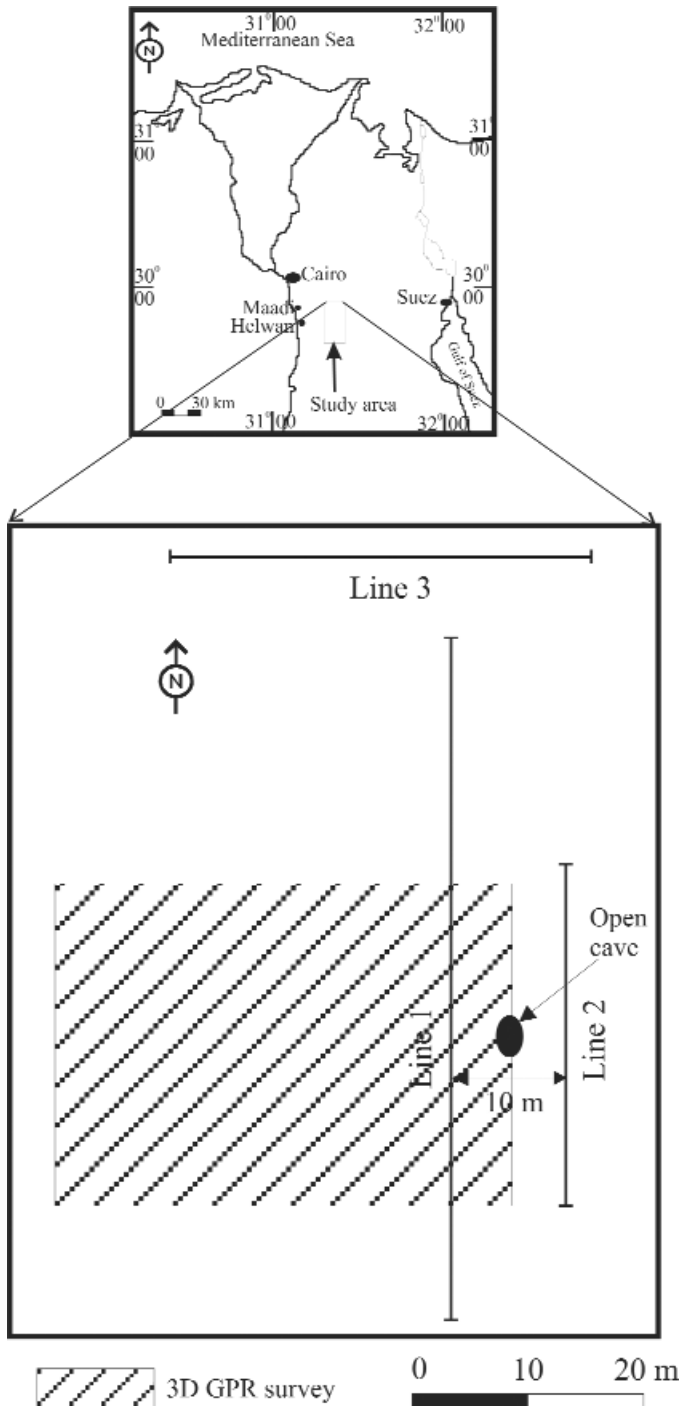


Figure 1. Location map of the study area.

rine unit composed of gravel, and a lower marine unit composed mainly of limestone with interbedded sandstone members.

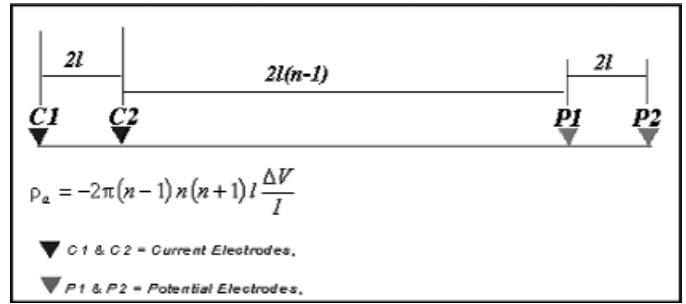


Figure 2. Electrode configurations for the dipole-dipole array for resistivity surveys.



Figure 3. Photograph of the cave outcrop and its dimensions.

GEOPHYSICAL DATA

RESISTIVITY IMAGING

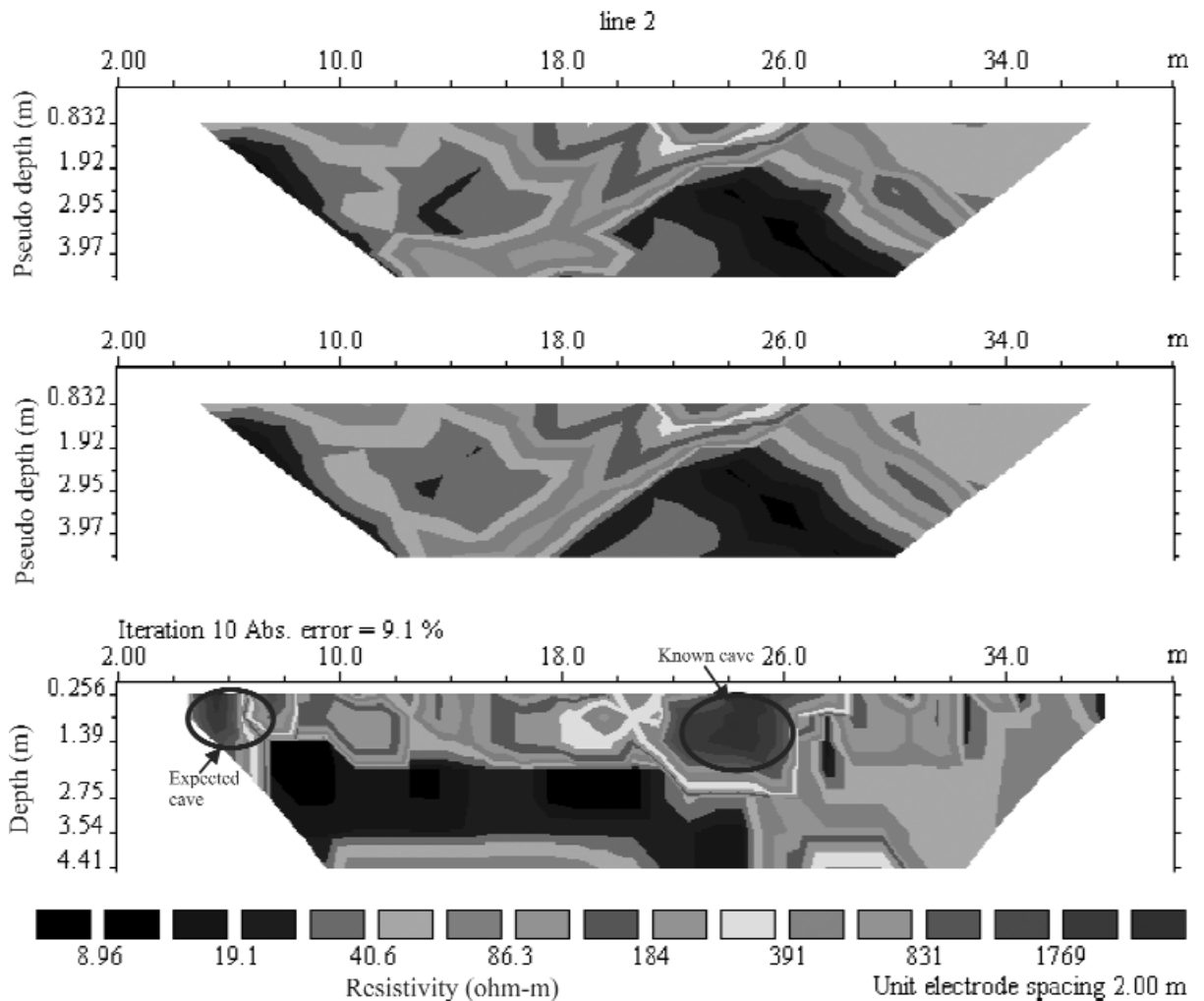
The concepts of electrical imaging are well described in the geophysical literature (e.g. LaBrecque *et al.*, 1996). Resistivity measurements are made for a large number of sets of four electrodes. Given these measurements, it is possible to solve numerically for a resistivity distribution that results in a set of calculated resistivity measurements that best fits with the measured response.

The dipole-dipole electrode configuration was used in this study. Figure 2 illustrates the layout for data acquisition. In this configuration, the apparent resistivity value is calculated according to the formula

$$\rho_a = -2\pi(n-1)n(n+1)l \frac{\Delta V}{I} \tag{1}$$

(see Figure 2 for symbol definitions). The array is widely used in resistivity and induced-polarization surveys, because of the low electromagnetic coupling between the current and potential circuits. Furthermore, this array is very sensitive to horizontal changes in resistivity. Hence it is good at mapping vertical structures such as dikes and cavities.

Figure 4.
Inverted dipole-dipole resistivity section along survey line L2; (top) measured apparent resistivity, (middle) calculated apparent resistivity, and (bottom) inverted model resistivity section.



The survey was conducted above an exposed cave with unknown extensions (Fig. 3). Resistivity measurements were acquired along three profiles, namely L1, L2, and L3 (Fig. 1). For L1 and L3, the electrodes were spaced 5 m apart, whereas for L2, 2 m. The data were collected using an IRIS Instruments Syscal-R2 system (IRIS, 1998).

The measured apparent resistivity data were inverted to create a resistivity model of the subsurface using iterative smoothness-constrained least squares (Loke and Barker, 1996; Loke, 1998). This scheme requires no previous knowledge of the subsurface; the initial-guess model is constructed directly from field measurements. A robust inversion (Claerbout and Muir, 1973) was used because it is suitable for detecting fractures and faults as well as for sharpening linear features such as faults, dikes, and contacts. The pseudosections of the measured and calculated apparent resistivity and the section of the inverted resistivity model for L2 are displayed in Figure 4 as an example. Figure 5 shows a collective 3-D view of the inverted resistivity models for the three profiles L1 to L3.

Generally, the resultant resistivity sections show that the site is characterized by a relatively moderate resistivity background (19–40 ohm-m). This can be referred to as the lithologic intercalation of marl (calcareous shale) with limestone.

The resistivity section of profile L2 (Fig. 4) shows two distinct areas of high resistivity centered approximately at 6- and 24-m horizontal distance. The first anomaly, >830 ohm-m, is at less than 1 m deep, and it appears in L1 at a different horizontal distance. The second one, >1760 ohm-m, extends deeper with a depth ranging from 0.5 to 3 m with a relatively large size. This anomaly also appears in L1. Such anomalies probably reflect cavities distributed in the limestone. Moreover, linear changes in the resistivity distribution that are obvious in section L3 are probably related to contacts between the hard limestone and the marl as well as other linear structures.

GROUND-PENETRATING RADAR

Ground-penetrating radar has become a common component of the standard array of geophysical techniques used to detect voids within limestone. The principles of the method are similar to those of seismic sounding, but in GPR the reflections come from objects and layers within the ground that alter the speed of transmission of the radar signal. Thus, air-filled voids and layers of water-saturated sediment are strong radar reflectors. The depth of penetration of the GPR depends on the frequency of the radar signal, as well as the electrical properties of the substrate.

Figure 5.
Three-dimensional view of the inverted resistivity sections for the survey lines.

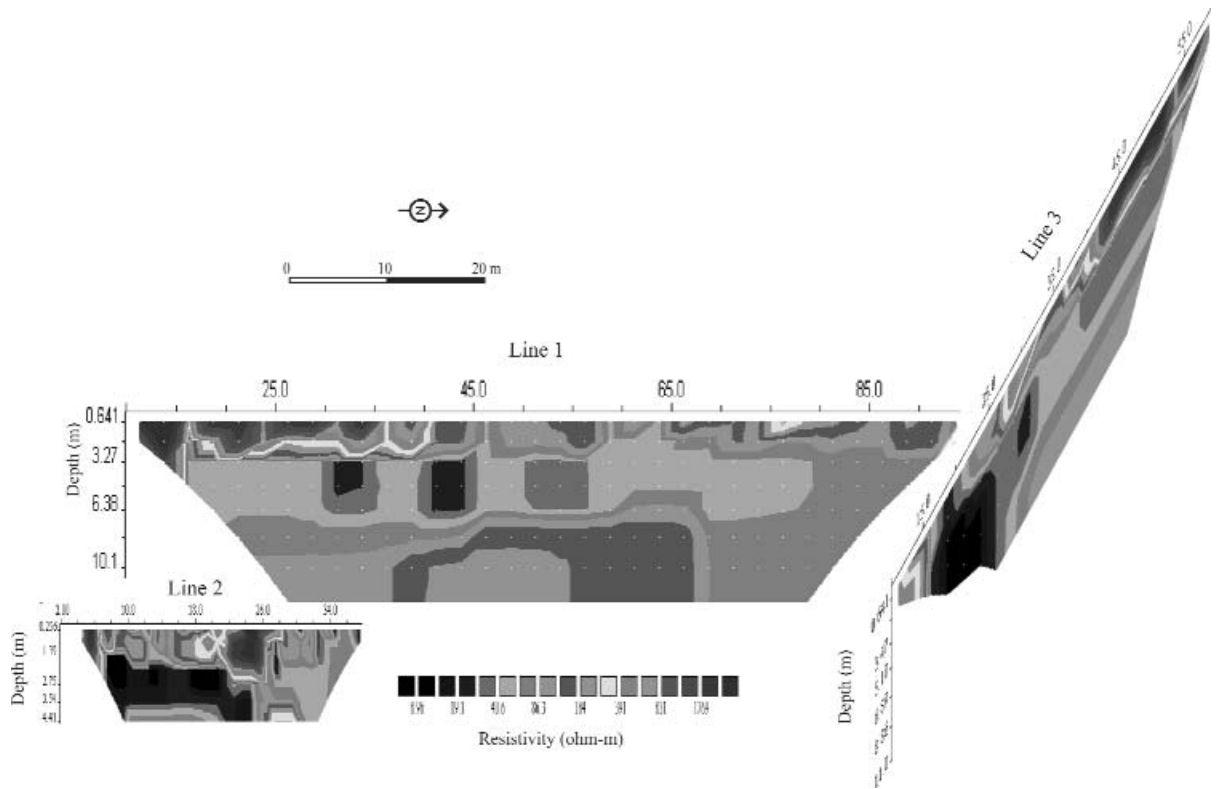
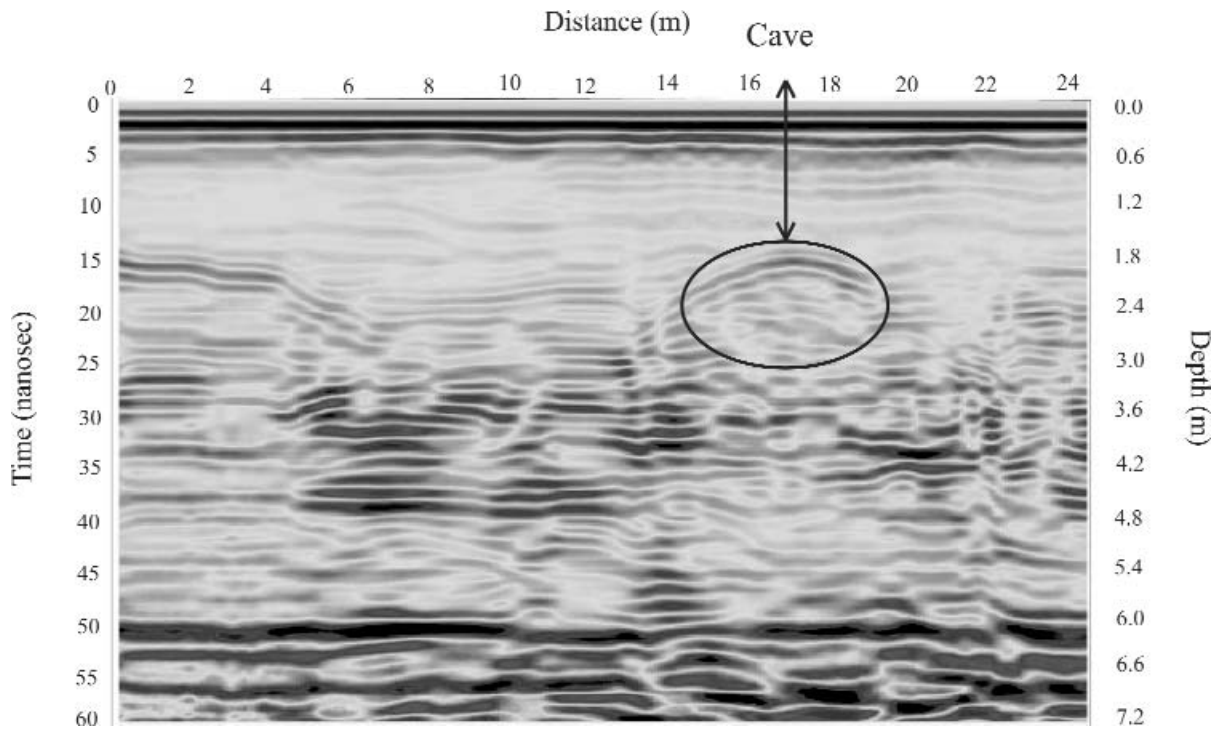


Figure 6.
Radar record along resistivity line L2, and over the cave.



GPR uses high-frequency electromagnetic waves to acquire subsurface information. The waves are radiated into the subsurface by an emitting antenna. When a wave strikes a suitable object, a portion of the wave is reflected back to a receiving antenna. Measurements are continuously recorded

with a resolution that is significantly higher than most other surface geophysical methods, providing a profile (a cross section) of subsurface conditions.

Figure 7.
Radar record
along resistivity
line L3.

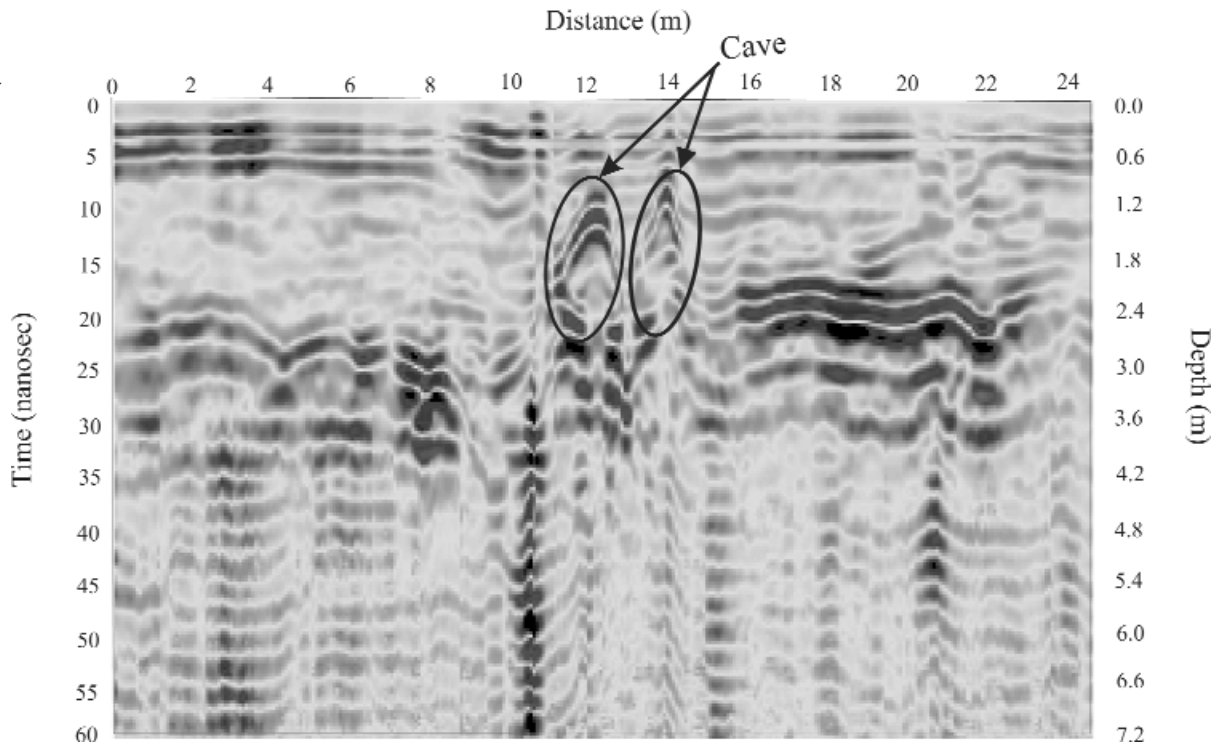
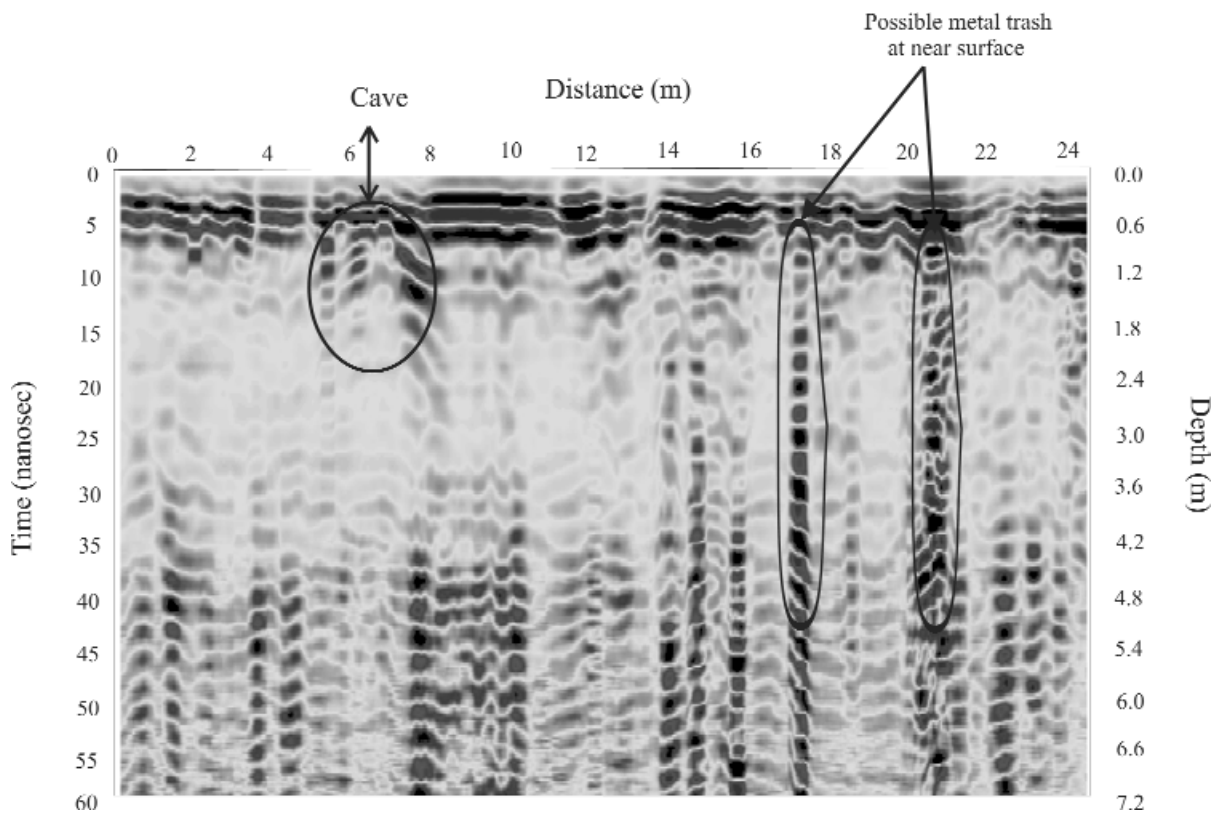


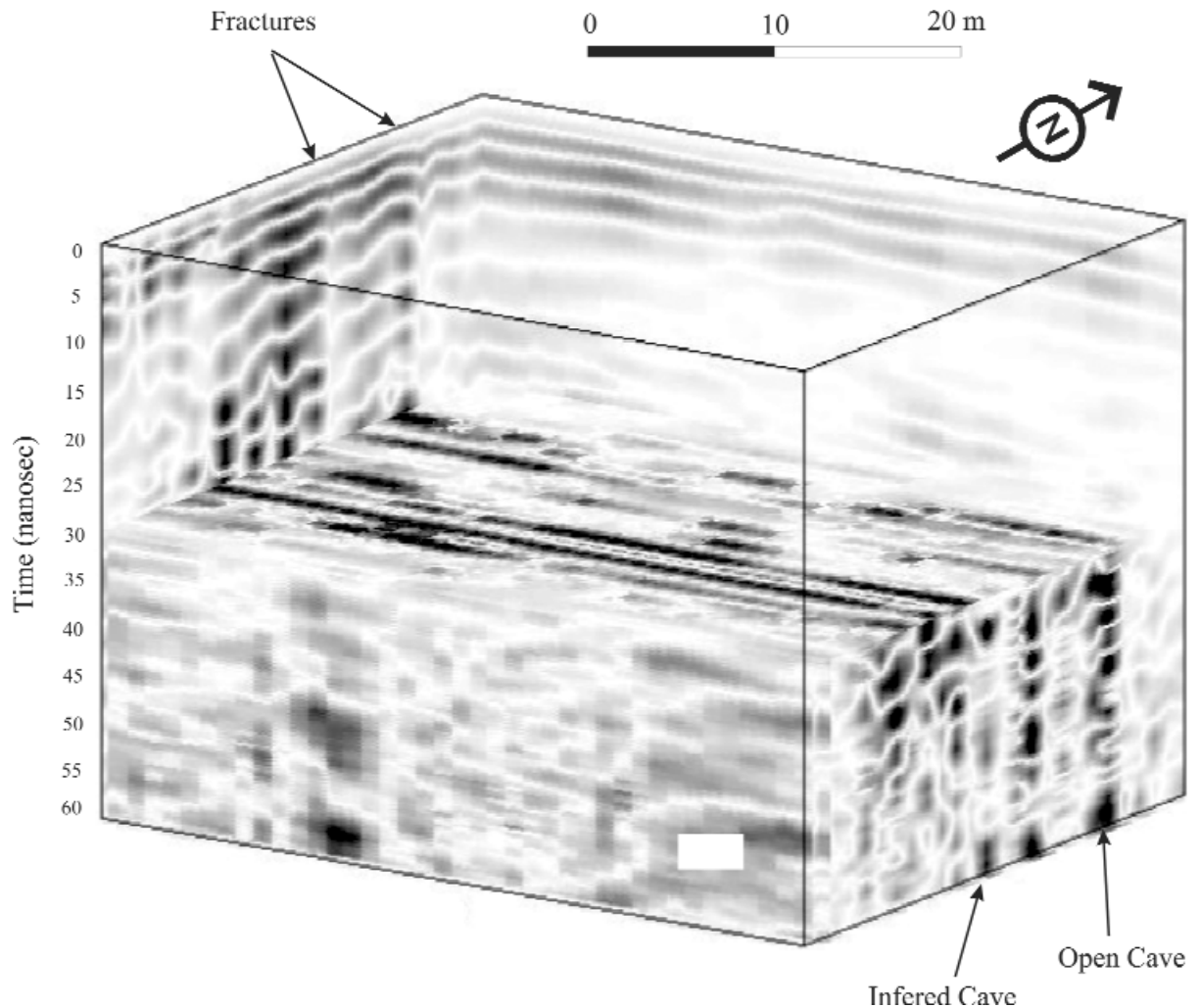
Figure 8.
Radar record
along resistivity
line L1.



In this paper, the GPR survey inspected the uppermost 10 m of the area. The GPR profiles were measured along the same three resistivity profiles (Fig. 1) using an SIR-2000 instrument equipped with a 200 MHz monostatic antenna applying time windows of 120 ns, with 20 scans per meter, and 512 samples

per scan. Additionally, 27 parallel profiles 41 m long and spaced 1 m apart extend from east to west for odd profiles, and from west to east for even (zigzag traverse mode). The profiles were measured using the same survey parameters to define the pathway of the cave system. The time over 60 ns was removed

Figure 9. Three-dimensional block depicting the position of the cave system.



where it was noisy. Whereas the data processing was conducted using the Reflex program (version 2.1.1), several processing steps were applied to each radar profile separately, such as background removal, band-pass filters (1- and 2-dimensional), median filter, and automatic-gain control. The band-pass filtering was applied in order to eliminate high-frequency components. The radar survey was conducted directly above a known cave system (Fig. 3) in order to determine its response to the radar signal, which may be used for delineating unknown cave systems in the study area in the future.

Figure 6 represents the processed radar record measured over the cave system along resistivity profile L2. Inspection of this figure shows a hyperbolic arc indicating the existence of the cave; the location and depth of the target can be determined from the vertex of the hyperbolic arc. The velocity of the electromagnetic wave is about 0.121 m ns^{-1} . The depth to the cave system is shown to be about 2 m, which correlates with the true depth of the cave. Keeping in mind the signature of the cave in the radar record, the other radar profiles can be interpreted. Inspection of the GPR section of Figure 7, which is measured perpendicular to the cave system and in line with L3, shows a hyperbolic feature at about 13 m from the starting point of the

profile and at a depth of about 1 m. It also shows that around the cave, significant fractures extend through the limestone, which may indicate that the cave system extends further. Moreover, the GPR section in Figure 8, which is measured inline with resistivity profile L1, shows that a substantial radar reflection anomaly is at a horizontal distance of between 5.5 and 7.5 m and about 1 m beneath the ground surface. Based on the shape and geometry of the anomalous radar features and the geologic condition of the study area, we believe that the area is characterized by subterranean voids that may be extensions of the known cave system.

THREE-DIMENSIONAL GPR TIME-SLICED IMAGE

Three-dimensional interpretations of ground-penetrating radar have been used to identify burials and other cultural features (Conyers and Goodman, 1997). In the past, the use of 3-D images has been restricted, because of the time required to conduct fieldwork over limited areas and the lack of satisfactory signal-processing software. The recent development of sophisticated software has enabled signal enhancement and improved pattern recognition on radar records. Figure 9 shows a 3-D block diagram of a $41 \times 27 \text{ m}$ grid area. Horizontal time-

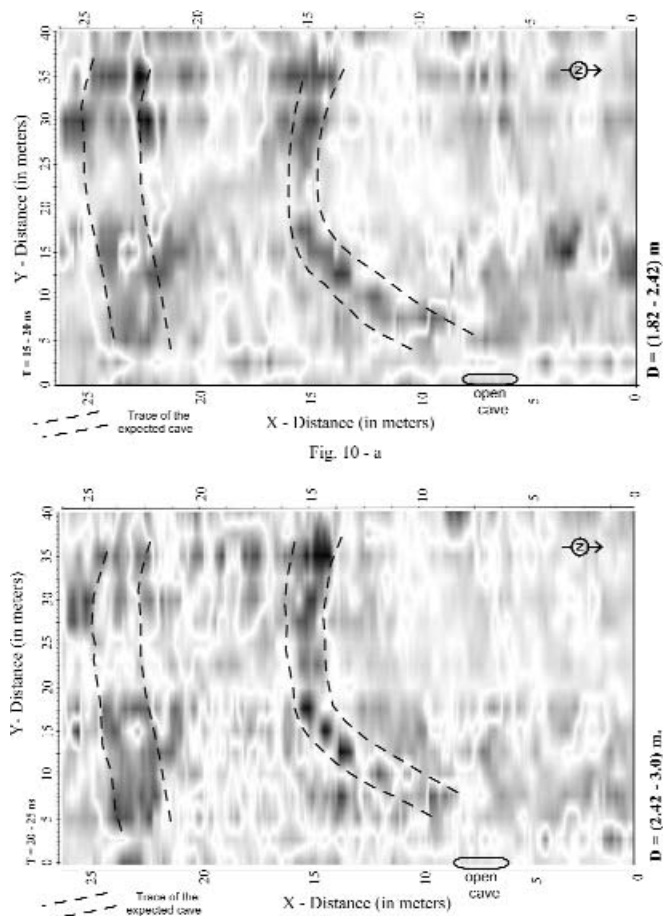


Figure 10. Horizontal time slices of radar data showing the trend of the cave. Figure 10-a depicts a 15–20 ns (1.82–2.45 m) slice and Figure 10-b depicts a 20–25 ns (2.42–3.00 m) slice.

slice maps (Figure 10) were made across the volume at depths ranging from approximately 1.8 m to 3.0 m. These depths were based on an assumed signal propagation velocity through the soil of 0.121 m ns^{-1} .

The top time slices from 15–20 ns (1.82–2.45 m) in Figure 10-a, and 20–25 ns (2.42–3.00 m) in Figure 10-b, show a series of hyperbolic reflectors aligned on adjoining radar records that form a linear pattern of high amplitudes (dark colors) at a uniform depth and orientated east to west. These reflectors are assumed to be the pathway of the cave system.

DISCUSSION AND CONCLUSION

The objective of this study was to investigate the caves and the shallow subsurface setting of the area to outline its geologic structures. Two-dimensional resistivity tomography using a dipole-dipole array and GPR data were collected and interpreted.

As the air-filled cavities have a near-infinite electrical resistance compared to the damp limestone, they produced readily recognizable anomalies. Based on the geophysical sig-

nature of the resistivity cross sections, two high-resistivity anomalous areas were detected. Additionally, a group of low resistivity zones were detected and interpreted as pockets of marl embedded in the limestone.

The processed GPR data elucidate a hyperbolic radar signal due to a cave at a depth of about 2 m, with a width of about 4 m, which is in good agreement with the known cave system in the study area. Moreover, some anomalous zones are delineated and are believed to reflect extensions of the cave system and other small karstic features.

Integrated interpretation of the acquired geophysical data along each profile is summarized in a schematic cross section (Fig. 11) showing the interpreted structures and the expected pathway of the cave system. With the existence of such caves, along with frequent large dynamite explosions used in a limestone quarry near the study area, the detected karstic features and fracture zones can be considered as the main risks for the new proposed housing development.

According to the results obtained from this study, we can conclude that ground-penetrating radar and electrical resistivity have proved to be effective tools for imaging subsurface cavities in limestone at shallow depths. On the other hand, natural cavities such as in this study occur in only a few types of rocks, and the rock surrounding natural cavities is often disturbed. This is particularly true in carbonate karstic environments where a cave is formed by the physical and chemical action of groundwater on the rock. In such an environment, fractures and the dissolution of rock surrounding a cave system creates a larger bulk anomalous volume than the cave itself. Fortunately, this helps geophysical methods to detect such caves easily. Consequently, we mainly find that the effective geophysical size of each cavity varies with the geologic environment, but it is usually larger than the real size of the cavity.

Finally, with the frequent massive dynamite explosions in the nearby limestone quarry, the detected fracture zones and karstic features can be considered as the main cause of likely future cracking at this site. Therefore, to increase the safety of homes in the area we recommend controlling the frequency and intensity of the dynamite explosions used at the limestone quarry.

ACKNOWLEDGEMENTS

The staff of the Egyptian National Research Institute of Astronomy and Geophysics (NRIAG) helped acquire the geophysical data using NRIAG facilities; sincere thanks to all of them. We are indebted to the staff of the Exploration Geophysical Laboratory in Kyushu University for their contributions and support during this work. We appreciate the thoughtful comments made by Dr. George Moore of Oregon State University, Dr. Paul Gibson of the University of Maynooth, and Dr. Richard Benson of Technos Inc for their constructive criticism that improved the paper. We appreciate efforts of Dr. Ira Sasowsky, for reading the final text. The Japan Society for the Promotion of Science (JSPS) supported the work of GE.

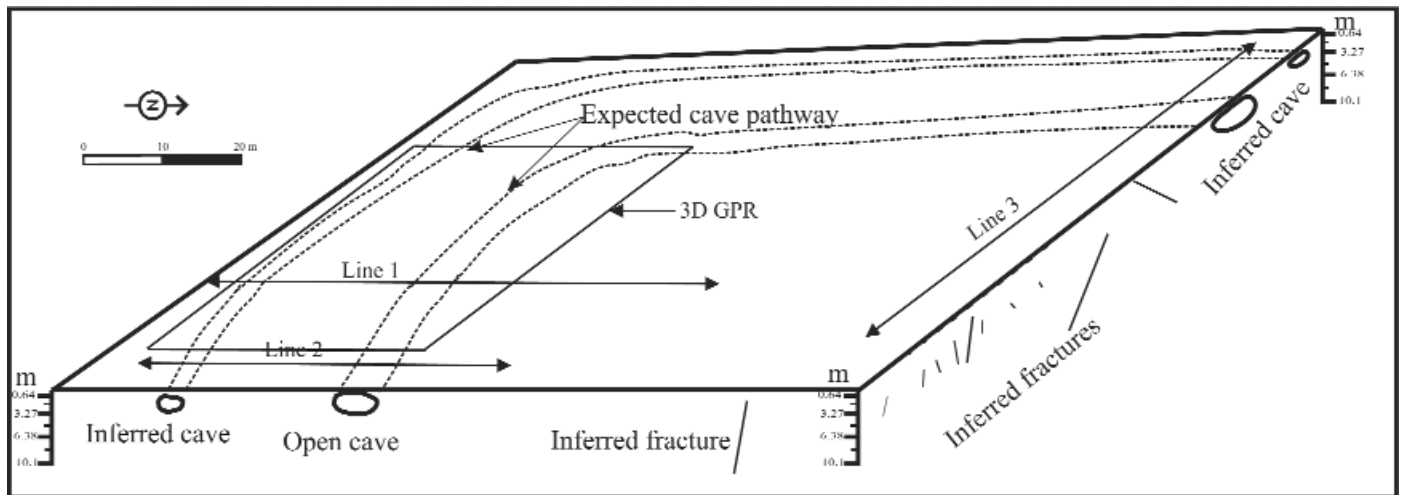


Figure 11. Three-dimensional conceptual view of the interpreted cross sections from the geophysical survey.

REFERENCES

- Claerbout, J., and Muir, F., 1973, Robust modeling with erratic data: *Geophysics*, v. 38, p. 826–844.
- Conyers, L., and Goodman, D., 1997, *Ground penetrating radar. An introduction for Archaeologists*: Walnut Creek, Altamira Press, 232 p.
- Elawadi, E., El-Qady, G., Salem, A., and Ushijima, K., 2001, Detection of cavities using pole-dipole resistivity technique: *Memoirs of the Faculty of Engineering, Kyushu Univ.*, v. 61, p. 101–112.
- Fisher, E., McMechan, G., and Annan, P., 1992, Acquisition and processing of wide-aperture ground-penetrating radar data: *Geophysics*, v. 57, p. 495–504.
- IRIS Instruments, 1998, *User manual of Syscal Junir-R2, multi-electrode system*: Orleans Cedex, 98 p.
- LaBrecque, D.J., Ramirez, A.L., Daily, W.D., Binley, A.M., and Schima, S.A., 1996, ERT monitoring of environmental remediation processes: *Measurement Science and Technology*, v. 7, p. 375–383.
- Loke, M.H., 1998, *RES2DINV, Rapid 2D resistivity and IP inversion using least-squares methods*, User manual: Austin, Tex., Advanced Geosciences, Inc., 66 p.
- Loke, M.H., and Barker, R.D., 1996, Rapid least-squares inversion of apparent resistivity pseudo sections by a quasi-Newton method: *Geophysical Prospecting*, v. 44, p. 131–152.
- Manzanilla, L., Barba, L., Chávez, R., Tejero, A., Cifuentes, G., and Peralta, N., 1994, Caves and geophysics: An approximation to the underworld of Teotihuacan, Mexico: *Archaeometry*, v. 36, p. 141–157.
- Noel, M., and Xu, B., 1992, Cave detection using electrical resistivity tomography: *Cave Science*, v. 19, p. 91–94.
- Palmer, L., 1959, Location of subterranean cavities by geoelectrical methods: *Mining Magazine (London)*, v. 91, p. 131–147.
- Reynolds, J.M., 1997, *An introduction to applied environmental geophysics*: West Sussex, John Wiley & Sons Ltd., 796 p.
- Said, R., 1962, *The geology of Egypt*: Amsterdam, Elsevier, 377 p.
- Smith D., 1986, Application of the pole-dipole resistivity technique in the detection of solution cavities beneath highways: *Geophysics*, v. 51, p. 833–837.
- Ushijima, K., Mizunaga, H., and Nagahama, S., 1989, Detection of cavities by the pole-dipole resistivity method: *Butsuri Tanasa (Geophysical Exploration of Japan)*, v. 40, p. 324–334.